Wind and Structures, Vol. 6, No. 4 (2003) 263-278
DOI: http://dx.doi.org/10.12989/was.2003.6.4.263

Effects of deck's width-to-depth ratios and turbulent flows on the aerodynamic behaviors of long-span bridges

Yuh-Yi Lin†, Chii-Ming Cheng‡ and Chao-Yuan Lan‡†

Department of Civil Engineering, Tamkang University, Tamsui, Taiwan 251, R.O.C.
(Received December 20, 2002, Revised May 26, 2003, Accepted August 20, 2003)

Abstract. This study investigates the effects of a bridge deck's width-to-depth (B/H) ratio and turbulence on buffeting response and flutter critical wind speed of long-span bridges by conducting section model tests. A streamlined box section and a plate girder section, each with four B/H ratios, were tested in smooth and turbulent flows. The results show that for the box girders, the response increases with the B/H ratio, especially in the vertical direction. For the plate girders, the vertical response also increases with the B/H ratio. However, the torsional response decreases as the B/H ratio increases. Increasing the B/H ratio and intensity of turbulence tends to improve the bridge's aerodynamic stability. Experimental results obtained from the section model tests agree reasonably with the calculated results obtained from a numerical analysis.

Keywords: width-to-depth ratio; turbulence; buffeting; flutter; section model; long-span bridge.

1. Introduction

The choice of bridge deck geometry is always a major concern for structural engineers. The design of long-span bridges is frequently dominated by aerodynamic considerations. The effects of deck shape on the aerodynamic behavior of long-span bridges are typically investigated in wind tunnel tests. Information useful for bridge design can be obtained from such studies. Scanlan and Tomko (1971) found that bluff bridge decks tend to undergo torsional flutter and be less aerodynamically stable than streamlined decks. Bienkiewicz (1987) studied the effects of geometry modification on bridge aerodynamics and found that streamlining a bridge deck can improve aerodynamic performance, with an increase in the flutter critical wind speed and a decrease in the vortex-induced response. Similar results have been also reported by other researchers. Nagao *et al.* (1993) studied two width-to-depth (B/H) ratios and concluded that a cross section with the greater B/H ratio induces smaller vortex-induced oscillation and has higher flutter wind speed. Matsumoto and his associates (1996, 1998) conducted tests on plate sections with various B/H ratios and found that a bridge deck with a smaller B/H ratio is less aerodynamically stable and tends to exhibit single-degree-of-freedom flutter. For rectangular sections, the critical B/H ratio that separates the classic flutter from the single-degree-of-freedom flutter is about 10~12.5. Based on past studies, a

† Associate Professor
‡ Professor
‡† Graduate Student

general conclusion can be drawn that the aerodynamic characteristics of a bridge deck section strongly depend on its geometry. Even a small geometrical modification may significantly change a deck's aerodynamic behavior. In the preliminary design of long-span bridges, as the deck width and shape are chosen, the optimal deck depth for improved aerodynamic behavior is desired. This need motivates this study, in which the effects of varying the depth of the cross-section of a deck (for a given deck width and shape) on the aerodynamic response are investigated. Two deck shapes - a streamlined box section and a plate girder section - each with four B/H ratios are considered.

In addition to the effect of the B/H ratio, the effects of turbulence on the deck buffeting response and the flutter wind speed are also examined. The results of previous studies on these effects on the aerodynamic stability of the bridge deck are inconclusive. Scanlan and Lin (1978) and Huston *et al.* (1988) found that the flutter derivatives obtained in turbulent flows were not significantly different from those obtained under laminar flow conditions. Wardlaw *et al.* (1983) found that turbulence reduces the vortex-induced response. However, it may or may not improve the aerodynamic stability of bridge decks. A theoretical study by Bucher and Lin (1990) showed that turbulence can have stabilizing or destabilizing influence on the aerodynamic stability. Scanlan (1997) considered the effects of coherence on aerodynamic stability. His results indicated that turbulence can increase the flutter wind speed. In the present study, the effects of turbulence are investigated in grid-generated homogeneous turbulent flows. The aerodynamic behavior of the two sections in these flows is discussed. The experimental results observed using the bridge section models are compared to those obtained by numerical analysis.

2. Basic theory

2.1. Flutter and buffeting forces

Consider a 2-DOF section model of bridge deck subjected to turbulent oncoming flow. Fluctuating wind loads that act on the deck can be represented by a combination of a motion- induced self-excited force and a buffeting force. The equations of motion in the lift (heave) and torsional (pitch) directions are expressed (Scanlan and Tomko 1971) as

$$m_y(\ddot{y} + 2\xi_y\omega_y\dot{y} + \omega_y^2 y) = L_f + L_b \tag{1}$$

$$I(\ddot{\alpha} + 2\xi_\alpha\omega_\alpha\dot{\alpha} + \omega_\alpha^2\alpha) = M_f + M_b \tag{2}$$

where the subscripts f and b denote respectively self-excited force and turbulence - induced buffeting force. The linearized form of the self-excited loading can be written as

$$L_f(t) = \frac{1}{2}\rho U^2(2B)(K)\left[H_1^*(K)\frac{\dot{y}(t)}{U} + H_2^*(K)\frac{B\dot{\alpha}(t)}{U} + KH_3^*(K)\alpha(t)\right] \tag{3}$$

$$M_f(t) = \frac{1}{2}\rho U^2(2B^2)(K)\left[A_1^*(K)\frac{\dot{y}(t)}{U} + A_2^*(K)\frac{B\dot{\alpha}(t)}{U} + KA_3^*(K)\alpha(t)\right] \tag{4}$$

where $K=B\omega/U$ is reduced frequency, ω is circular frequency, B is deck width, ρ is air mass

density, U is average wind speed, y, α represent, lift and torsional displacements, respectively. $H_j^*(K)$, $A_j^*(K)$ $(j=1,3)$ are the flutter derivatives. Based on the quasi-steady theory, the buffeting forces on a bridge deck section in the vertical and torsional directions can be simplified as follows:

$$L_b(t) = \frac{1}{2}\rho U^2 B\left\{C_L(\alpha_0)\frac{2u(x,t)}{U} + \left[\frac{dC_L}{d\alpha}\bigg|_{\alpha=\alpha_0} + \frac{A}{B}C_D(\alpha_0)\right]\frac{w(x,t)}{U}\right\} \tag{5}$$

$$M_b(t) = \frac{1}{2}\rho U^2 B^2\left\{\left[C_M(\alpha_0) + C_D(\alpha_0)\frac{Ar}{B^2}\right]\frac{2u(x,t)}{U} + \frac{dC_M}{d\alpha}\bigg|_{\alpha=\alpha_0}\frac{w(x,t)}{U}\right\} \tag{6}$$

where u, w are velocity fluctuations in the drag and lift directions, C_D, C_L, C_M are the drag, lift and torstional wind force coefficients, α_0 is the mean wind angle of attack, A is the deck's projected area on the vertical axis, and $\boldsymbol{r}$ is the distance of deck mass center from the effective axis of rotation.

2.2. Buffeting response of full bridge deck

Structural and aerodynamic coupling effects are neglected hereafter to simplify the interpretation of the results of section model tests. The resulting equation of the vertical motion of the ith mode can be stated as follows (Scanlan 1987):

$$M_{yi}^*[\ddot{X}_{yi}(t) + 2\tilde{\xi}_{yi}(2\pi n_{yi})\dot{X}_{yi}(t) + (2\pi n_{yi})^2 X_{yi}(t)] = \int_0^L \phi_i^y(x)L_b dx \tag{7}$$

where M_{yi}^*, X_{yi}, $\dot{X}_{yi}$, $\ddot{X}_{yi}$, n_{yi}, $\phi_i^y(x)$ are respectively the generalized mass, displacement, velocity, acceleration, natural frequency, and the mode shape of the ith modal contribution. L is the deck span, $\tilde{\xi}_{yi}$ is the effective damping ratio and defined as follows:

$$\tilde{\xi}_{yi} = \xi_{yi} - \frac{\rho B^2\int_0^L(\phi_i^y(x))^2 dx}{2M_{yi}^*}H_1^*(K)\frac{n}{n_{yi}} \tag{8}$$

where n is the frequency. Based on the random theory, the variance of the vertical displacement at section x_p contributed by mode i can be expressed by

$$\sigma_{yi}^2 = \frac{(\phi_i^y(x_p))^2}{16\pi^4 n_{yi}^4 (M_{yi}^*)^2}\int_0^L\int_0^L \phi_i^y(x_p)\phi_i^y(x_q)dx_p dx_q \int_0^\infty \frac{S_{L_pL_q}^C(n)}{\left\{\left[1-\left(\frac{n}{n_{yi}}\right)^2\right]^2 + 4\tilde{\xi}_{yi}\left(\frac{n}{n_{yi}}\right)^2\right\}}dn \tag{9}$$

where $S_{L_pL_q}^C$ is the cross force spectrum between nodes p and q. Assume the excitation has broad band nature, Eq. (9) can be simplified as

$$\sigma_{yi}^2 = \frac{(\phi_i^y(x_p))^2}{16\pi^4 n_{yi}^4 (M_{yi}^*)^2} \frac{\pi(2\pi n_{yi})}{4\zeta_{yi}} S_{L_p L_p}(n_{yi}) \lambda_L \int_0^L \int_0^L \phi_i^y(x_p)\phi_i^y(x_q) dx_p dx_q \tag{10}$$

where ζ_{yi} is the damping ratio and can be obtained from Eq. (8) by replacing n with n_{yi}, λ_L is the non-dimensional span-wise correlation length of force spectrum. Introducing the following dimensionless parameters,

$$n^* = n_{yi}B/U,\ M^{**} = M_{yi}^* / \left(\rho B^2 \int_0^L (\phi_i^y(x))^2 dx\right),\ S_L^* = n_{yi} S_{L_p L_p}(n_{yi}) / \left(\frac{1}{2}\rho U^2 B\right)^2$$

then Eq. (10) can be rewritten as

$$\sigma_{yi}^2 = (\phi_i^y(x_p))^2 \frac{B^2}{\left(\int_0^L (\phi_i^y(x))^2 dx\right)^2} \left(\int_0^L \int_0^L \phi_i^y(x_p)\phi_i^y(x_q) dx_p dx_q\right) \frac{\pi^2 S_L^* \lambda_L}{128 (n^*)^4 \zeta_{yi} (M^{**})^2} \tag{11}$$

Assume the force can be reasonably simulated and a section model constructed based on the similarity requirements, the relationship between the vertical response of the model and that of the prototype is given by

$$\frac{(\sigma_y^2)_m}{(\sigma_{yi}^2)_{pr}} = \frac{(\phi_i^y(x))_m^2 \left[\left(\int_0^L (\phi_i^y(x))^2 dx\right)^2\right]_{pr} \left(\int_0^l \int_0^l \phi_i^y(x_p)\phi_i^y(x_q) dx_p dx_q\right)_m (B^2)_m}{(\phi_i^y(x))_{pr}^2 \left[\left(\int_0^l (\phi_i^y(x))^2 dx\right)^2\right]_m \left(\int_0^L \int_0^L \phi_i^y(x_p)\phi_i^y(x_q) dx_p dx_q\right)_{pr} (B^2)_{pr}} \tag{12}$$

where the subscripts m and pr represent the section model and the prototype, respectively, l is the length of the section model. Similarly, the relationship between the torsional response of the model and that of the prototype is given by

$$\frac{(\sigma_\alpha^2)_m}{(\sigma_{\alpha i}^2)_{pr}} = \frac{(\phi_i^\alpha(x))_m^2 \left[\left(\int_0^L (\phi_i^\alpha(x))^2 dx\right)^2\right]_{pr} \left(\int_0^l \int_0^l \phi_i^\alpha(x_p)\phi_i^\alpha(x_q) dx_p dx_q\right)_m}{(\phi_i^\alpha(x))_{pr}^2 \left[\left(\int_0^l (\phi_i^\alpha(x))^2 dx\right)^2\right]_m \left(\int_0^L \int_0^L \phi_i^\alpha(x_p)\phi_i^\alpha(x_q) dx_p dx_q\right)_{pr}} \tag{13}$$

3. Experimental apparatus

The section model test was conducted in the Tamkang University Wind Tunnel. The wind tunnel has a working section of 1.5 m(W)×1.8 m(H)×7.4 m(L). The length of bridge deck model is 1.5 m. Two controlling parameters were selected in the wind tunnel test - the width-to-depth ratio (B/H) and the oncoming turbulence. Two types of decks, one of the box girder type (model 1 series) and the other of the plate girder type (model 2 series), were selected to investigate the effects of B/H ratios on bridge aerodynamics. For each type of deck, four section models, with B/H ratios from 5

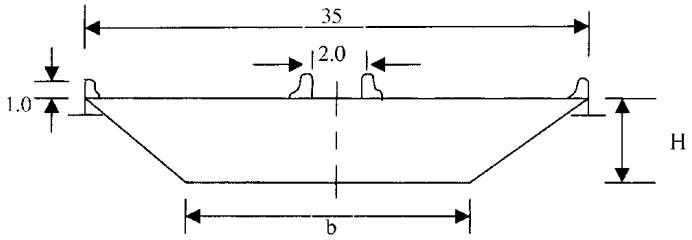

Model	1-1	1-2	1-3	1-4
b(cm)	27.7	25.4	21.8	15.4
H(cm)	1.75	2.4	3.2	5.0

Fig. 1 Geometry of section models (box girders)

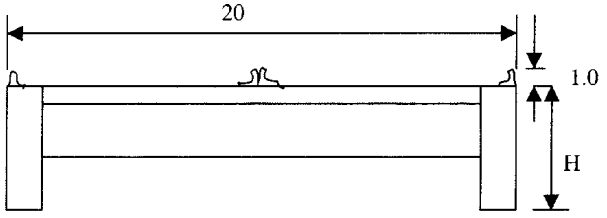

Model	2-1	2-2	2-3	2-4
H(cm)	1.5	2	3	5

Fig. 2 Geometry of section models (plate girders)

to 20, were built and tested. The geometry of these decks is shown in Figs. 1-2. The mass and frequency of each section were nearly the same to compare fairly the aerodynamic behavior of the sections. The sectional properties of the prototype and these section models are listed in Table 1. In the first part of this study, all eight models were tested under smooth flow and under a turbulent flow with a longitudinal turbulence intensity of 10%.

The second part of this study investigates the influence of turbulence on the aerodynamic behavior of the bridge. Two sets of grids were used to generate five homogeneous turbulent flow fields for model testing. The turbulence intensity varies from 1% in the smooth flow up to 16% in the flow

Table 1 Sectional properties of the prototype and section models

Properties \ Model	Prototype	Model 1	Model 2
Width (m)	35 (20 for model 2)	0.35	0.2
Mass (kg/m)	25400	2.54	2.54
Polar mass moment of inertia (kg-m^2/m)	3,600,000	0.036	0.036
Vertical frequency (Hz)	0.167	5.13	5.14
Torsional frequency (Hz)	0.368	12.15	12.21
Torsional-to-vertical frequency ratio	2.2	2.37	2.37

Table 2 Properties of turbulent flows

Flow field	*s*	*a*	*b*	*c*	*d*	*e*
Turbulence intensity (%)	1	5	8	10	12	16

field *e*. The integral length scales vary from 20 to 50 cm. Table 2 lists the flow conditions. In this part of the study, only model 1-3 (B/H=11) and model 2-3 (B/H=6.7) were used for wind tunnel testing.

In each test case, the vertical and torsional responses at different wind speeds were measured; the measured results were then substituted into Eq. (12) or (13) to predict the responses of the prototype bridge. The interpreted results, obtained from the section model tests, are compared to the analytical results, based on the wind force coefficients and flutter derivatives.

4. Experimental results

To fairly compare the results, the measured vertical and torsional responses are plotted against the reduced frequency U/nB in which the frequency n is the natural frequency of the torsional mode.

4.1. Effects of B/H ratios

4.1.1. Box girder series

Figs. 3 and 4 plot the torsional and vertical responses of model 1 versus the reduced velocity, respectively, under smooth flow conditions. Fig. 3 shows that the vortex-induced torsional responses are significant for each model, and that the model with the smaller B/H ratio has the larger response. For these box sections, the flutter wind speed increases with the B/H ratio. These results

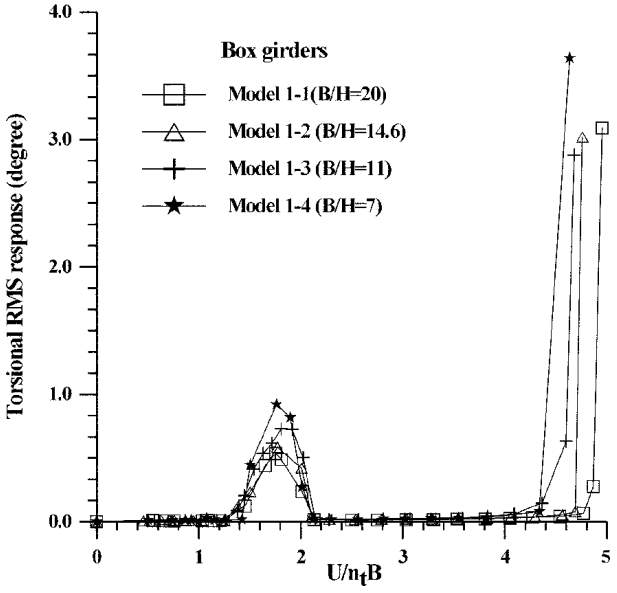

Fig. 3 Torsional RMS response of box girders under smooth flow

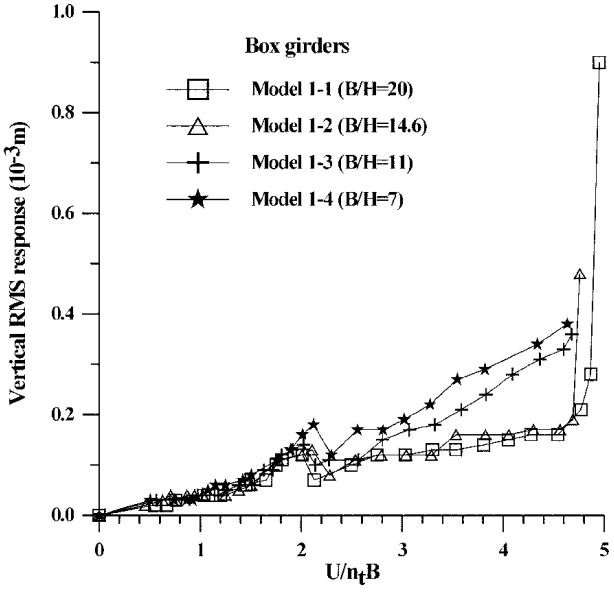

Fig. 4 Vertical RMS response of box girders under smooth flow

are expected because the shallower sections are better streamlined and aerodynamically stable. Fig. 4 shows that the vortex-induced vertical response is less significant than the torsional response. At high wind speeds, the vertical responses of models 1-1 and 1-2 rapidly increase, but those of models 1-3 and 1-4 do not. This result indicates that the sections with larger B/H ratios exhibit stronger coupling effects than those with smaller B/H ratios.

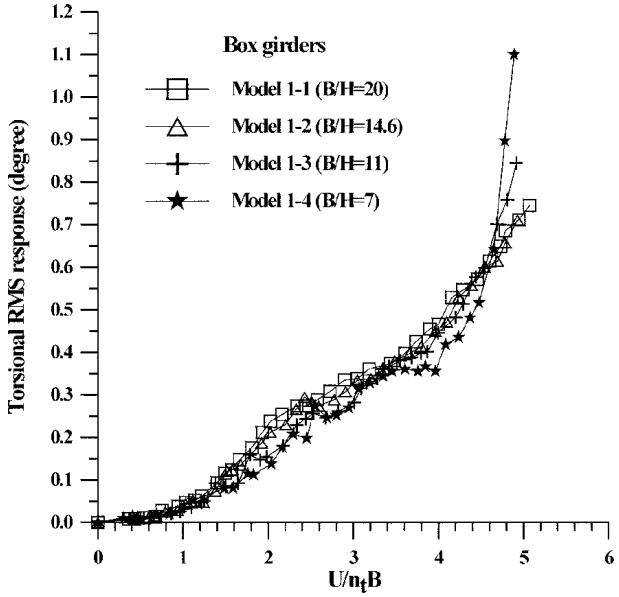

Fig. 5 Torsional RMS response of box girders under turbulent flow

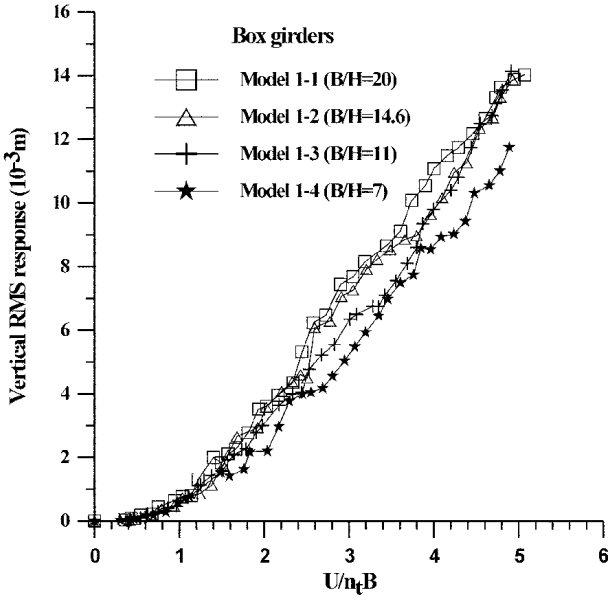

Fig. 6 Vertical RMS response of box girders under turbulent flow

Table 3 Aerodynamic behaviors of model series 1(box girders)

Model	1-1	1-2	1-3	1-4
B/H ratio	20	14.6	11	7
Vertical response (mm, U/nB=3.5)	8.8	8.6	7.4	7.1
Torsional response (degree, U/nB=3.5)	0.38	0.38	0.37	0.36
Flutter wind speed (m/s, smooth flow)	20.3	19.9	19.7	18.4

Figs. 5 and 6 plot the torsional and vertical responses of model 1 versus the reduced velocity, respectively, in turbulent flow with an intensity of 10%. Fig. 5 reveals no significant vortex-induced torsional response, indicating that turbulence reduces vortex-induced vibration. The torsional buffeting response slightly increases with the B/H ratio, although not significantly. A comparison between Figs. 3 and 5 indicates that turbulence can delay the onset of aerodynamic instability. Fig. 6 shows that the vertical buffeting response, similar to the torsional response, increases with B/H ratio.

Table 3 presents the effects of the B/H ratios of the box sections on the aerodynamic behaviors. The buffeting response increases with the B/H ratio, especially in the vertical direction. The trend of the vortex-induced response is reversed; that is, a section with a smaller B/H ratio has a larger response. With regard to aerodynamic stability, the flutter wind speed increases with the B/H ratio and the turbulence is beneficial to stability.

4.1.2. Plate girder series

Figs. 7 and 8 plot the torsional and vertical responses of model 2 versus the reduced velocity, respectively, under smooth flow conditions. Fig. 7 reveals no significant vortex-induced torsional responses of any model. The flutter wind speed increases with the B/H ratio of the plate girder sections, as with

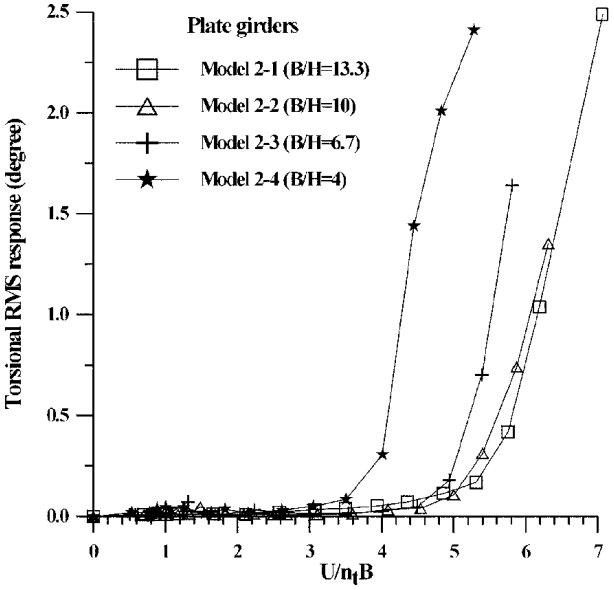

Fig. 7 Torsional RMS response of plate girders under smooth flow

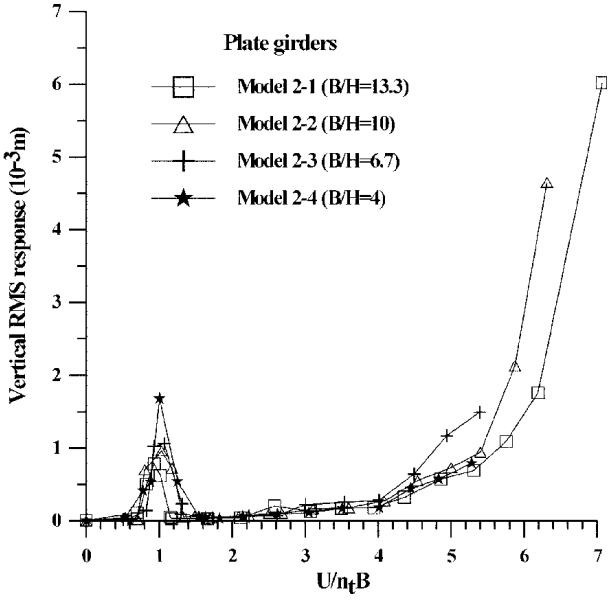

Fig. 8 Vertical RMS response of plate girders under smooth flow

that of the box sections. The results in Fig. 8 indicate that the vortex-induced vertical responses are more significant than the torsional responses; the section with the smaller B/H ratio exhibits a larger response. This result implies that plate girder sections are apt to exhibit vertical vortex-induced vibration, unlike box sections, in which torsional vortex-induced vibrations are more significant. The vertical responses of plate girder sections with larger B/H ratios rapidly increase because of the more significant coupling effects.

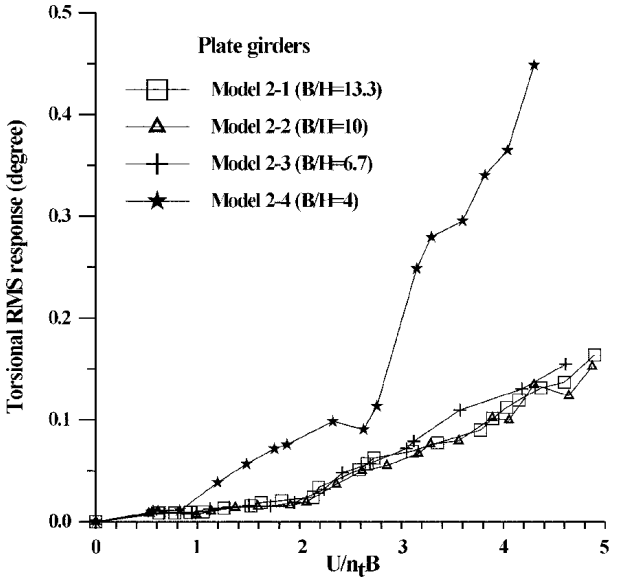

Fig. 9 Torsional RMS response of plate girders under turbulent flow

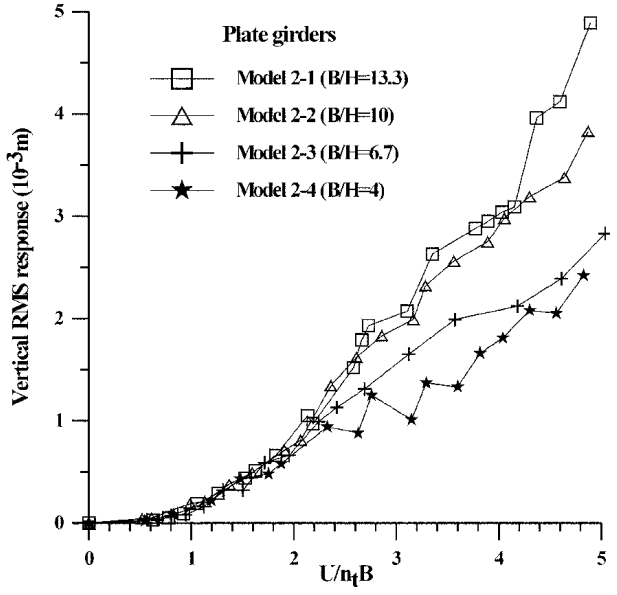

Fig. 10 Vertical RMS response of plate girders under turbulent flow

Figs. 9 and 10 plot the torsional and vertical responses of model 2 versus the reduced velocity, respectively, under turbulent flow with an intensity of 10%. Fig. 9 indicates that the torsional buffeting response decreases as the B/H ratio increases. This trend is the reverse of that exhibited by the mode1 1 series. Fig. 10 shows that the vortex-induced vertical responses diminish, indicating that turbulence reduces vortex-induced vibration. This figure also shows that the vertical buffeting response, unlike the torsional response, increases with the B/H ratio.

Table 4 Aerodynamic behaviors of model series 2(plate girders)

Model	2-1	2-2	2-3	2-4
B/H ratio	13.3	10	6.7	4
Vertical response (mm, U/nB=3.5)	2.72	2.51	1.94	1.34
Torsional response (degree, U/nB=3.5)	0.08	0.08	0.12	0.29
Flutter wind speed (m/s, smooth flow)	14.1	13.2	12.1	9.8

Table 4 presents the effects of the B/H ratio of a plate girder section on its aerodynamic behavior. The trend is the vertical buffeting response increases with the B/H ratio; however, the torsional response decreases as the B/H ratio increases. The section with the smaller B/H ratio has the larger vortex-induced vertical response. The flutter wind speed increases with the B/H ratio and turbulence promotes aerodynamic stability.

4.2. Effects of turbulence

The effects of turbulence on the vertical and torsional buffeting responses of the closed box girder are similar to those of the plate girder. These effects are shown in Figs. 11-14. Higher free stream turbulence tends to enhance responses in the vertical and torsional directions. Since the increase in

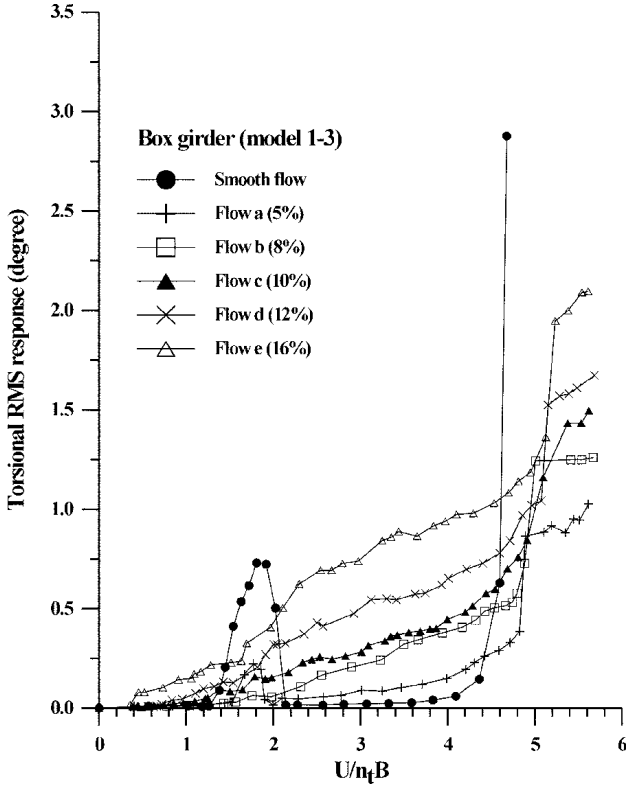

Fig. 11 Torsional RMS response of model 1-3 under different turbulent flows

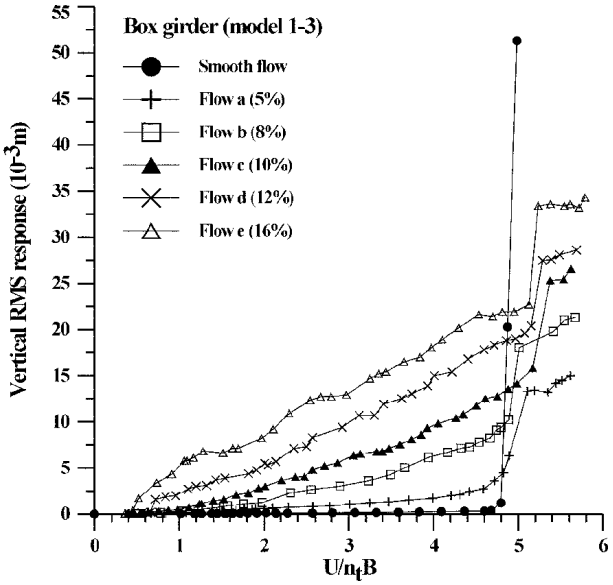

Fig. 12 Vertical RMS response of model 1-3 under different turbulent flows

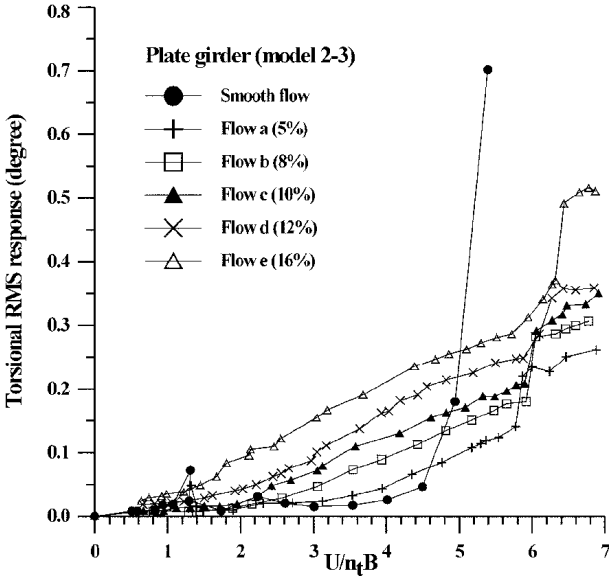

Fig. 13 Torsional RMS response of model 2-3 under different turbulent flows

the torsional response under the turbulent flow is not as sharp as that under smooth flow when flutter occurs, the determination of the flutter onset velocity under the turbulent flow may not be as precise as that in smooth flow. However, the flutter onset velocity is taken here as the velocity at which the torsional response starts to increase rapidly. Table 5 lists the results. The results show that turbulence can enhance the aerodynamic stability of both types of sections, and that the flutter onset wind speed increases slightly, but not obviously, with the intensity of turbulence.

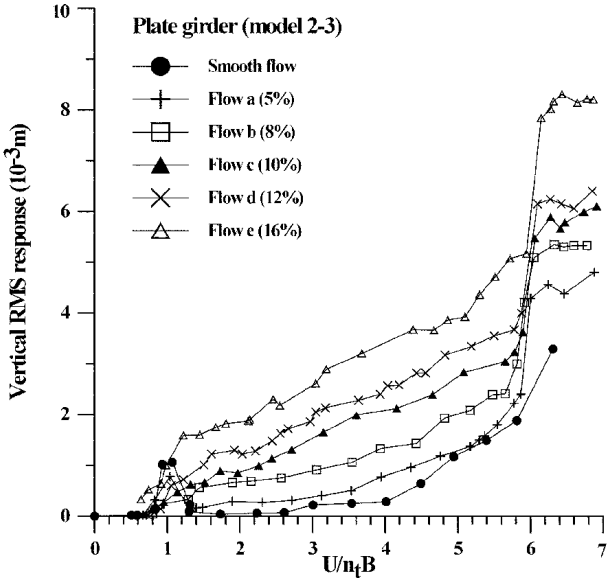

Fig. 14 Vertical RMS response of model 2-3 under different turbulent flows

Table 5 Flutter wind speeds under turbulent flows

Flow field	Smooth flow	*a*	*b*	*c*	*d*	*e*
Model 1-3 (m/s)	19.7	20.2	20.5	20.9	21.0	21.2
Model 2-3 (m/s)	12.1	14.1	14.5	14.4	14.4	15.4

4.3. Buffeting response and flutter wind speed of the prototype bridge

A cable-stayed bridge with a major span of 720 m and two side spans, each of 220 m, is used for this study. The box girder with the B/H ratio of 11 (model 1-3) is used as the deck section. Fig. 15 shows the geometry of the bridge. Table 1 presents the calculated natural frequencies of the first lift and torsional modes of this bridge. The lift and torsional coefficients C_L and C_M, used for buffeting

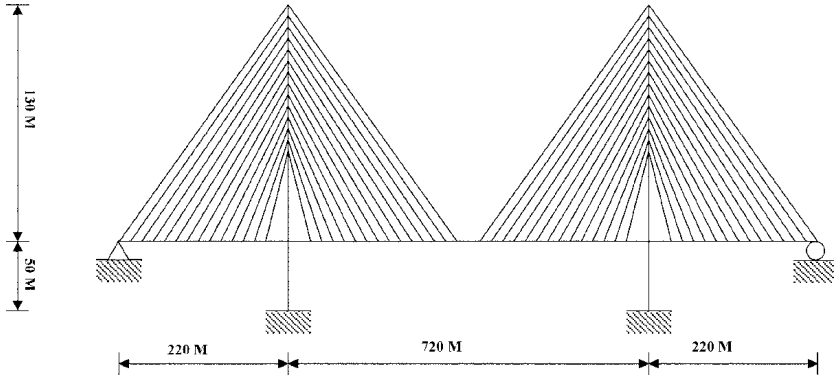

Fig. 15 Geometry of the prototype bridge

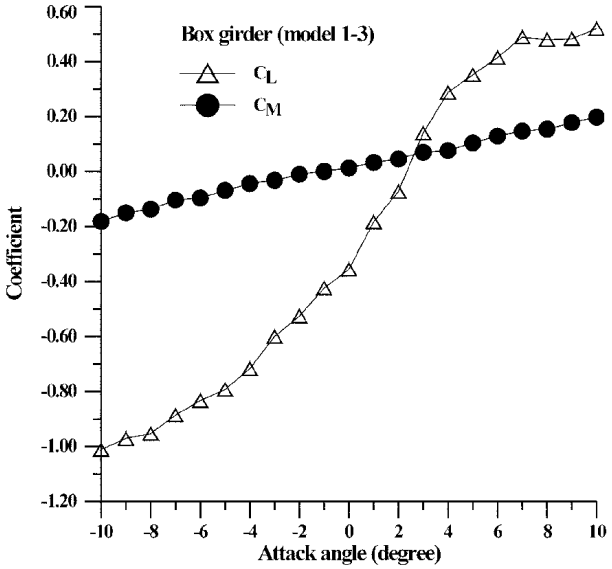

Fig. 16 Lift and torsional coefficients

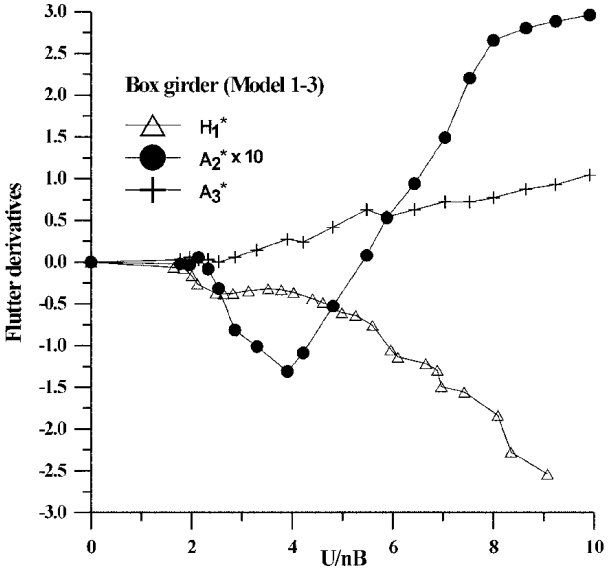

Fig. 17 Flutter derivatives

calculations, are shown in Fig. 16. Some of the flutter derivatives are shown in Fig. 17. The vertical and torsional buffeting responses of the prototype bridge, based on Eqs. (12)-(13) and the measured responses of model 1-3, are shown in Figs. 18-19. A multi-mode approach (Jain *et al.* 1996), based on static force coefficients and flutter derivatives, was employed to calculate the buffeting response. In this numerical analysis, the structural and aerodynamic coupling are considered and the aerodynamic admittance is set to be unity. These numerical results are also shown in Figs. 18-19. A comparison of the results indicates that the discrepancies between them are within a reasonable range. Table 6 presents the flutter onset

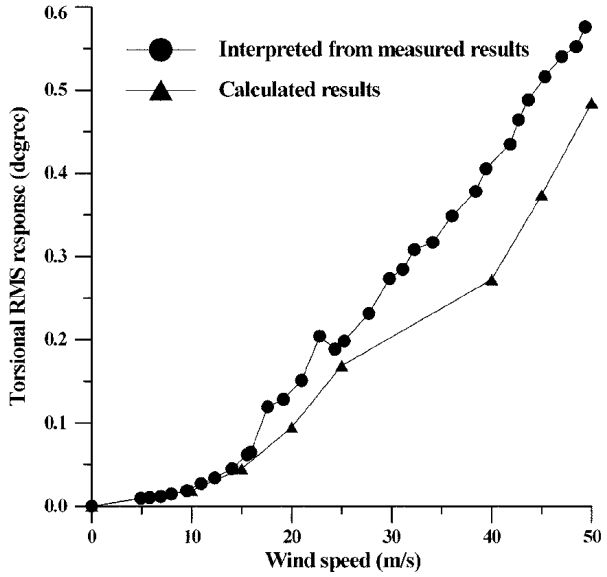

Fig. 18 Comparison of the torsional RMS responses interpreted from measured results and calculated results

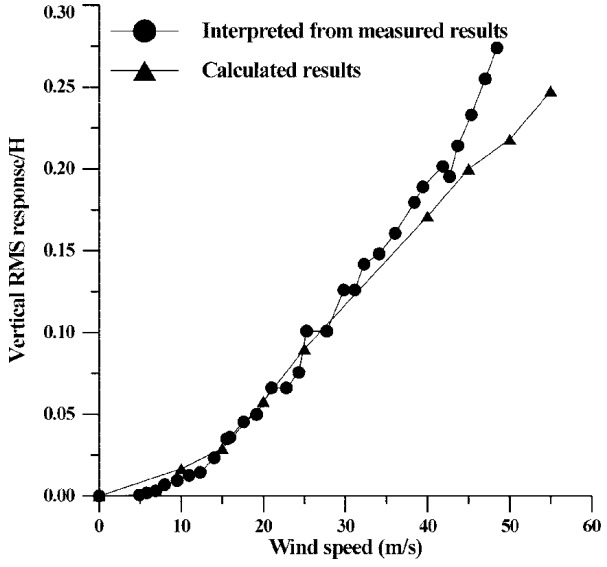

Fig. 19 Comparison of the vertical RMS responses interpreted from measured results and calculated results

Table 6 Flutter wind speeds of the prototype bridge under turbulent flows

Flow field	Smooth flow	*a*	*b*	*c*	*d*	*e*
Interpreted from test results (m/s)	59.2	60.7	61.4	62.7	63.03	63.7
Calculated results (m/s)	59.8	61.5	62.7	-	65.4	67.3

speeds of the prototype bridge, obtained from the tests and by numerical analysis. A comparison of the results shows that the flutter onset wind speeds obtained by the two methods are in good agreement.

5. Conclusions

Based on wind tunnel tests on several section models under various flow conditions, the following conclusions can be drawn:

(1) The buffeting response of the box girders increases with the B/H ratio, especially in the vertical direction. The vertical buffeting response of the plate girders also increases with the B/H ratio; however, the torsional buffeting response decreases as the B/H ratio increases.
(2) The vortex-induced response of both types of deck sections decreases as the B/H ratio increases. The turbulence reduces the vortex-induced response.
(3) For both types of deck sections, the flutter wind speed increases with the B/H ratio. This phenomenon is more significant for the plate girder deck than the closed box girder deck. The flutter wind speed of both types of sections can be increased by turbulence.
(4) Comparisons of the aerodynamic behaviors between both types of sections indicate that the closed box girder deck has a significantly higher flutter wind speed than the plate girder deck. Therefore, the closed box girder is more aerodynamically stable.
(5) The buffeting responses of the prototype bridge, interpreted from section model tests and obtained by numerical analysis, are within a reasonable range. The flutter wind speeds of the bridge obtained by the two methods agree well.

Acknowledgments

The writers gratefully acknowledge the financial support of part of this work by the National Science Council (R. O. C.) under the grant NSC 90-2211-E-032-009.

References

Bienkiewicz, B. (1987), "Wind tunnel study of effects of geometry modification on aerodynamics of a cable stayed bridge deck", *J. Wind Eng. Ind. Aerodyn.*, **26**, 325-339.
Bucher, C.G. and Lin, Y.K. (1990), "Effects of wind turbulence on motion stability of long-span bridges", *J. Wind Eng. Ind. Aerodyn*, **36**, 1355-1364.
Huston, D.R., Bosch, H.R. and Scanlan, R.H. (1988), "The effect of fairing and of turbulence on the flutter derivatives of a notably unstable bridge deck", *J. Wind Eng. Ind. Aerodyn*, **29**, 339-349.
Jain, A., Jones, N.P. and Scanlan, R.H. (1996), "Coupled aeroelastic and aerodynamic response analysis of long-span bridges", *J. Wind Eng. Ind. Aerodyn*, **60**, 69-80.
Matsumoto, M. and Abe, K. (1998), "Role of coupled derivative on flutter instabilities", *Wind Struct.*, **1**, 175-181.
Matsumoto, M., Kbayashi, Y. and Shirato, H. (1996), "The influence of aerodynamic derivative on flutter", *J. Wind Eng. Ind. Aerodyn*, **60**, 227-239.
Nagao, F., Utsunomiya, H., Oryu, T. and Manabe, S. (1993), "Aerodynamic efficiency of triangular fairing on box girder bridge", *J. Wind Eng. Ind. Aerodyn*, **74**, 73-90.
Scanlan, R.H. and Lin, W.H. (1978), "Effects of turbulence on bridge flutter derivatives", *J. Eng. Mech. Div.*, **104**, ASCE, 719-733.
Scanlan, R.H. and Tomko, J.J. (1971), "Airfoil and bridge deck flutter derivative", *J. Eng. Mech. Div.*, **97**, ASCE, 1717-1737.
Scanlan, R.H. (1987), "Interpreting aeroelastic models of cable-stayed bridges", *J. Eng. Mech.*, **113**, ASCE, 555-575.
Scanlan, R.H. (1997), "Amplitude and turbulence effects on bridge flutter derivatives", *J. Struct. Eng.*, **123**, ASCE, 232-236.
Wardlaw, R.L., Tanaka, H. and Utsunomiya, H. (1983), "Wind tunnel experiments on the effects of turbulence on the aerodynamic behavior of bridge road decks", *J. Wind Eng. Ind. Aerodyn*, **14**, 247-257.

CC